

Motion-based prediction of external forces and moments and back loading during manual material handling tasks

Supplementary materials

1 Appendix A

External forces prediction

The biomechanical model used in the current study was composed of 16 rigid segments (pelvis, lower trunk, upper trunk, head, clavicles, upper arms, lower arms + hands, upper legs, lower legs and feet) linked by 15 joints corresponding to 37 rotational degrees of freedom (3 for the pelvis/lower trunk joint, 3 for the lower trunk/upper trunk joint, 3 for the neck, 3 for each the upper trunk/clavicles joint, 3 for each shoulder, 2 for each elbow, 3 for each hip, 1 for each knee and 2 for each ankle) (Figure 1). The thorax was connected to the ground with a free joint (6-degrees of freedom joint) and constituted the floating-base. From motion capture data (range of motion-type motion), the geometrical parameters were subject-specific calibrated by an optimization-based method (Muller et al., 2016). Body segment inertial parameters (BSIP) were computed from an anthropometric table (Dumas et al., 2007).

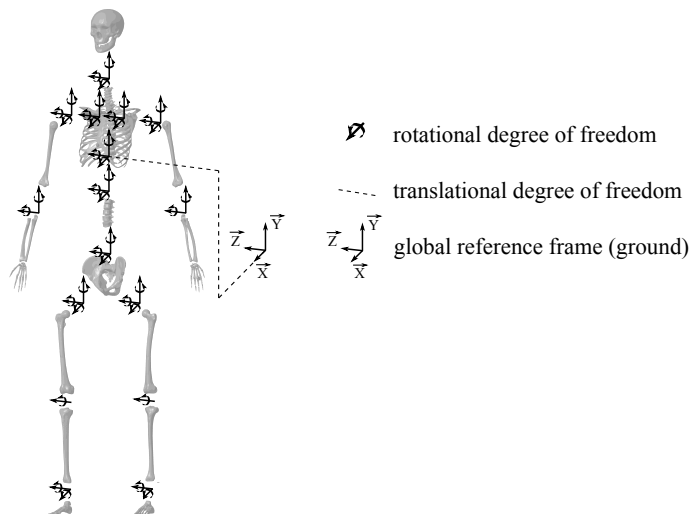


Figure 1: Representation of the biomechanical model.

From the positions of the 48 anatomical landmarks (estimated with the positions of the 12 rigid clusters), the inverse kinematics problem consisted in computing the vector of generalized joint coordinates \mathbf{q} . For each time step i , the sum of squared distances between measured and model-determined anatomical landmarks positions were minimized (1) using the global optimization method proposed by Lu and O’connor (1999).

$$\min_{\mathbf{q}(i)} \sum_{m=1}^{n_m} \|\mathbf{X}_{mod,m}(\mathbf{q}(i)) - \mathbf{X}_{exp,m}(i)\|^2 \quad (1)$$

Where $\mathbf{X}_{mod,m}(\mathbf{q}(i))$ is the coordinates of anatomical landmarks m , located on the model, obtained by forward kinematics and $\mathbf{X}_{exp,m}(i)$ is the coordinates of the experimental anatomical landmarks m .

The joint coordinate trajectories were composed of the set of joint coordinates obtained for each time step. Then, these trajectories were filtered using a 4-th order Butterworth low pass filter with a cut-off frequency of 5 Hz and no phase shift. Joint velocities and accelerations were calculated with finite difference method.

For the prediction method, a set of discrete contact points was defined on the biomechanical model (corresponding to the hypothesized contact points between the subject and the environment): N_f points under each foot and N_h points on each hand. For this study $N_f = 14$ and $N_h = 11$ were chosen (Figure 2). These points were defined to map the contact area in the same way as in previous studies (Fluit et al., 2014; Skals et al., 2017).

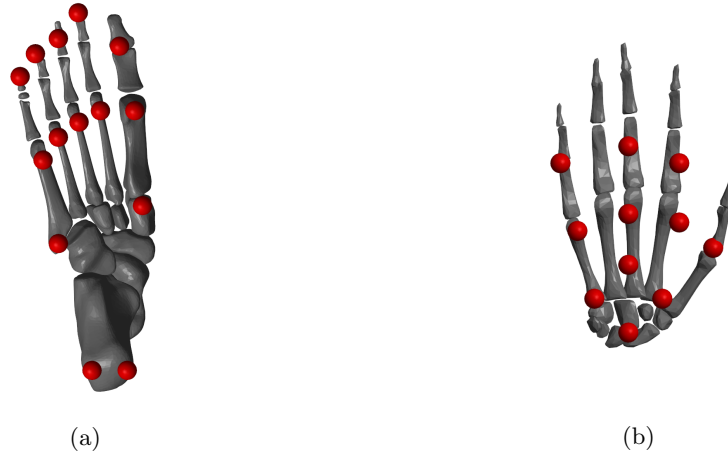


Figure 2: Discrete contact points defined on the biomechanical model. (a): 14 contact points under each foot; (b): 11 contact points on each hand.

Handling tasks were composed of 4 different successive phases (Figure 3): 1) the pre-grip, from the initial contact between the hands and the load to the final contact between the load and the grip support; 2) the transfer, from the end of the pre-grip to the initial contact between the load and the destination support; 3) the post-deposit, from the end of the transfer to the final contact between the hands and the load; 4) the return, from the end of the post-deposit to the beginning of the pre-grip phase. During the pre-grip and the post-deposit phases, the load was in contact with the subject's hands and load support. As no information was available about the contact between the load and its support, the motion-based prediction method did not allow to correctly predict the external forces in these phases. The detection of the phases were manually done by using a video observation.

The transfer and the return phases were processed in two different steps. During the return phase (the subject did not carry the load), the prediction method was a classical GRF&M prediction method from the equations of motion applied to the subject. Thus, at each instant, the external efforts were the solution of the optimization problem (2), solved with a Sequential Quadratic Programming (SQP) method.

$$\begin{aligned}
 \min_{\mathbf{F}} \quad & \sum_{i=1}^{2N_f} \|\mathbf{F}_i\|^2 \\
 \text{s.t.} \quad & \mathbf{M}_s(\mathbf{q})\ddot{\mathbf{q}} + \mathbf{C}_s(\mathbf{q}, \dot{\mathbf{q}}) + \mathbf{G}_s(\mathbf{q}) + \mathbf{E}_s = \mathbf{0}; \\
 & \forall i \in \llbracket 1, 2N_f \rrbracket, \mathbf{F}_i \leq \mathbf{F}_i^{max}
 \end{aligned} \tag{2}$$

Where, by isolating the biomechanical model, $\mathbf{M}_s(\mathbf{q})$ is the inertia matrix, $\mathbf{C}_s(\mathbf{q}, \dot{\mathbf{q}})$ is the centrifugal and Coriolis force vector, $\mathbf{G}_s(\mathbf{q})$ is the gravity force vector, \mathbf{E}_s is the generalized external force vector and \mathbf{F}_i^{max} is the vector containing the maximal forces available for the contact point i . The dynamics equations applied on the subject were obtained using a recursive Newton-Euler algorithm (Featherstone, 2014) with a bottom-up approach. Respecting these dynamics equations was ensured by imposing forces and moments as zero in the 6-degrees of freedom joint linking the ground and the floating-base. At each instant, we ensured that each actuator was sufficiently close to the floor and almost without motion

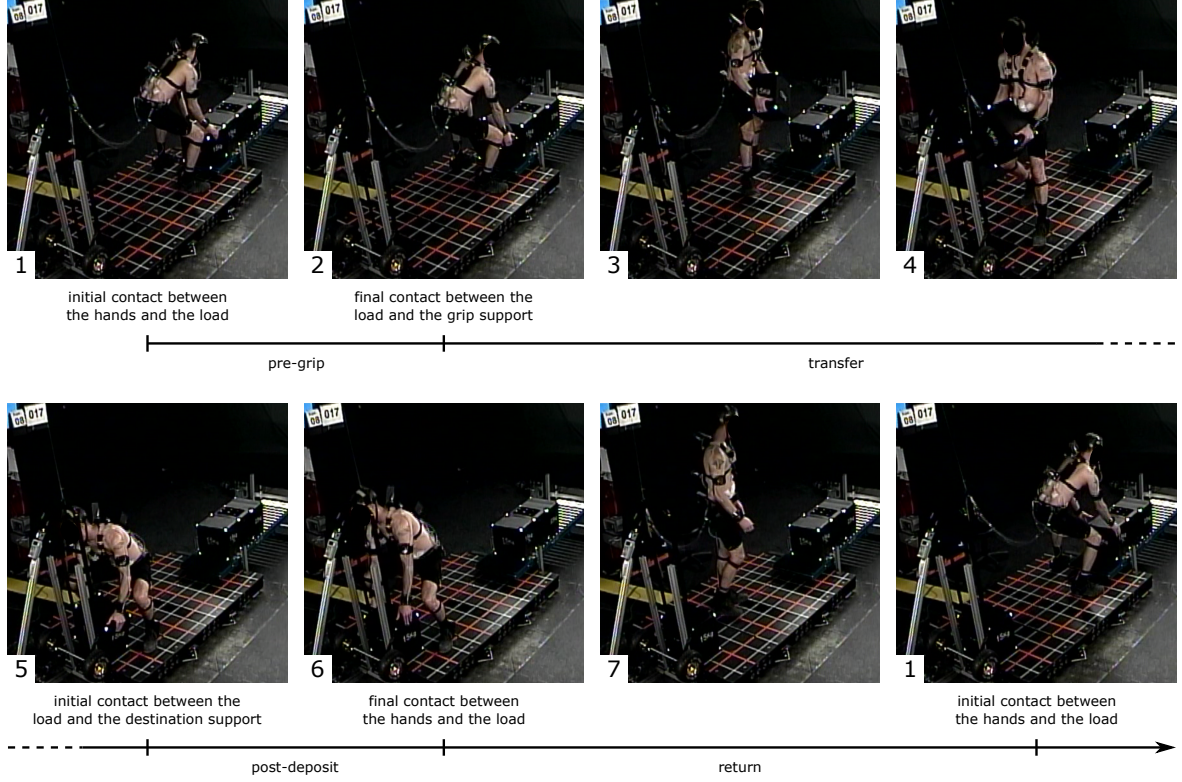


Figure 3: Different phases of the experimental tasks consisting in transferring four boxes one by one from a conveyor to a hand trolley and back again.

(Fluit et al., 2014; Skals et al., 2017). The distance and velocity thresholds were respectively 0.02 m and 0.8 m/s. When a contact point was respecting the thresholds, the associated force was limited to 0.4 BW (Body Weight) and had to respect the Coulomb's law of friction. A friction coefficient of 0.5 was used here (Skals et al., 2017; Bonnet et al., 2017). The external force vector \mathbf{E}_s contained the external efforts \mathbf{F}_i applied on the feet.

During the transfer phase (the subject carried the load), the prediction method took into account simultaneously the equations of motion applied to the subject and the equations of motion applied to the load. Thus, at each instant, the external efforts were the solution of the optimization problem (3), solved with a SQP method.

$$\begin{aligned}
 \min_{\mathbf{F}} \quad & \sum_{i=1}^{2(N_f+N_h)} \|\mathbf{F}_i\|^2 \\
 \text{s.t.} \quad & \mathbf{M}_s(\mathbf{q})\ddot{\mathbf{q}} + \mathbf{C}_s(\mathbf{q}, \dot{\mathbf{q}}) + \mathbf{G}_s(\mathbf{q}) + \mathbf{E}_s = \mathbf{0}; \\
 & \mathbf{M}_l(\mathbf{q})\ddot{\mathbf{q}} + \mathbf{C}_l(\mathbf{q}, \dot{\mathbf{q}}) + \mathbf{G}_l(\mathbf{q}) + \mathbf{E}_l = \mathbf{0}; \\
 & \forall i \in \llbracket 1, 2(N_f + N_h) \rrbracket, \mathbf{F}_i \leq \mathbf{F}_i^{max}
 \end{aligned} \tag{3}$$

Where, by isolating the load, $\mathbf{M}_l(\mathbf{q})$ is the inertia matrix, $\mathbf{C}_l(\mathbf{q}, \dot{\mathbf{q}})$ is the centrifugal and Coriolis force vector, $\mathbf{G}_l(\mathbf{q})$ is the gravity force vector and \mathbf{E}_l is the generalized external force vector. The maximal forces for contact points on the feet were the same as defined above. The external efforts vector \mathbf{E}_s contained the external forces applied on the feet and the external efforts vector \mathbf{E}_l contained the external forces applied on the hands. As was done for the return phase, the dynamics equations applied on the subject were obtained using a recursive Newton-Euler algorithm (Featherstone, 2014) with a bottom-up approach. Respecting these dynamics equations was ensured by imposing forces and moments as zero in the 6-degrees of freedom joint linking the ground and the floating-base.

All data were processed with CusToM (Customizable Toolbox for Musculoskeletal simulation (Muller

et al., 2019)) in Matlab[®], in which was implemented the GRF&M prediction method. CusToM is a toolbox enabling musculoskeletal analyses based on inverse dynamics approaches with a high level of customization of the analyses. Additional developments were done to take into account the equations of motion of the load.

2 Appendix B

Example of L5/S1 joint moment estimation

Figure 4 shows a representative example of a flexion/extension L5/S1 joint moment estimated from the predicted and from the measured data. For this example, the RMSE is 13.9 N (± 6.1) and the rRMSE is 4.4 % (± 1.9). These values are in the same order of magnitude of the mean values for all the tasks of all the subjects.

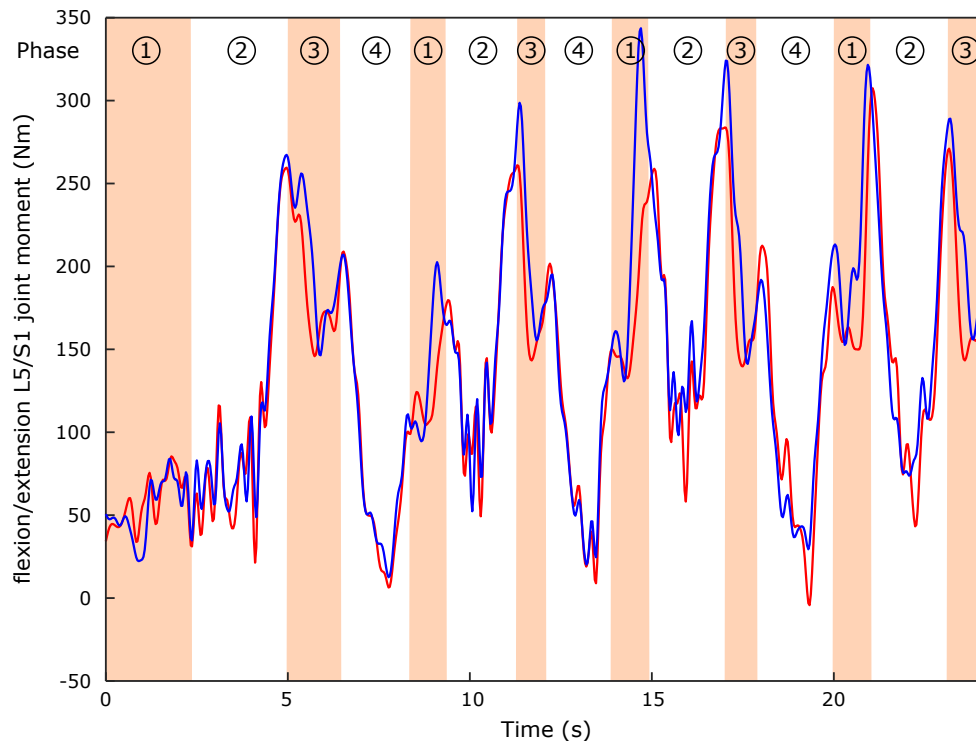


Figure 4: Representative example of flexion/extension L5/S1 joint moments estimated from the predicted (blue curve) and from the measured (red curve) data. The task consists in transferring four boxes one by one from a hand trolley to a conveyor. Phase 1 corresponds to the pre-grip, phase 2 corresponds to the transfer, phase 3 corresponds to the post-deposit and phase 4 corresponds to the return. The subject was a male novice worker of 43 years old, 1.80 m and 102 kg.

The task consists in transferring four boxes one by one from a hand trolley to a conveyor. As the deposits were already on the ground level, L5/S1 joint moments were between 200 Nm and 300 Nm according to the transferred box at this instant (end of the phases 2). Due to the use of a hand trolley, the height of the grips decreased for each box where the L5/S1 joint moment increases from approximately 50 Nm to 300 Nm at the beginning of phase 2. During the return (phase 1), the moment is about 200 Nm when there is an important trunk flexion (close to the grip or deposit phases) and under 50 Nm when the subject moves without the box.

Important prediction errors are observed in the areas displayed in orange, corresponding to the pre-grip and the post-deposit phases. During these phases, the load was in contact with the subject's hands and also with its support. As no information is available about the contact between the load and its support, the proposed method did not allow to correctly predict the external forces in these phases.

References

- Bonnet, V., Azevedo-Coste, C., Robert, T., Fraisse, P., and Venture, G. (2017). Optimal external wrench distribution during a multi-contact sit-to-stand task. *IEEE Transactions on Neural Systems and Rehabilitation Engineering*, 25(7):987–997.
- Dumas, R., Cheze, L., and Verriest, J.-P. (2007). Adjustments to mcconville et al. and young et al. body segment inertial parameters. *Journal of biomechanics*, 40(3):543–553.
- Featherstone, R. (2014). *Rigid body dynamics algorithms*. Springer.
- Fluit, R., Andersen, M. S., Kolk, S., Verdonschot, N., and Koopman, H. F. (2014). Prediction of ground reaction forces and moments during various activities of daily living. *Journal of biomechanics*, 47(10):2321–2329.
- Lu, T.-W. and O’connor, J. (1999). Bone position estimation from skin marker co-ordinates using global optimisation with joint constraints. *Journal of biomechanics*, 32(2):129–134.
- Muller, A., Germain, C., Pontonnier, C., and Dumont, G. (2016). A simple method to calibrate kinematical invariants: application to overhead throwing. In *ISBS-Conference Proceedings Archive*, volume 33.
- Muller, A., Pontonnier, C., Puchaud, P., and Dumont, G. (2019). Custom: a matlab toolbox for musculoskeletal simulation. *Journal of Open Source Software*, 4(33):1–3.
- Skals, S., Jung, M. K., Damsgaard, M., and Andersen, M. S. (2017). Prediction of ground reaction forces and moments during sports-related movements. *Multibody system dynamics*, 39(3):175–195.